Comparative Study on the Impact of Chemistry Mechanisms and Radiation Modeling on Extinction and CO Formation in Unsteady Laminar Flamelet Modeling with Low Scalar Dissipation Rates

Kruljevic B.[1,] *, Stankovic I.[1], Merci B.[1]

[1] *Ghent University, Ghent, Belgium*
**Corresponding author's email: Boris.Kruljevic@UGent.be*

ABSTRACT

This study fits within the context of turbulent combustion modelling in fires. Compared to jet flames, fire configurations are typically characterized by low scalar dissipation rates and strong influence of buoyancy. Furthermore, when it comes to extinction, particularly interesting is a low scalar dissipation rate limit, where extinction occurs due to radiative heat losses. This motivates the present study where different radiation approaches are tested at low scalar dissipation rates, as well as different chemical mechanisms for methane combustion, since chemistry plays an important role when it comes to extinction. The following chemical mechanisms are used: a one-step global mechanism [1], the 'Smooke' mechanism [2], the 'ARM2' [3] mechanism and the 'GRI3' [4] mechanism. Each of these chemical mechanisms is further combined with two different radiation models, an optically thin model with radiative properties based on the RADCAL model [5], and a model with a prescribed constant radiative fraction as obtained from the experiments. The impact of radiation is quantified through comparison to cases without radiation. The turbulent combustion model is the Conditional Moment Closure (CMC) method, where no transport in physical space is considered and thus the flow field simulations are not required. As the transport effects in physical space are not considered, an unsteady laminar flamelet model [6] is effectively applied and referred to as "CMC-0D", as it corresponds to a 0D reactor flow computation. The settings for fuel and the oxidizer correspond to the UMD line burner [7], for which a range of cases has been studied experimentally, with variable degrees of local extinction due to an increase of the N_2 concentration in the oxidizer. The fuel is pure methane. The values of O_2 mass fraction at extinction obtained with the GRI3, ARM2 and Smooke mechanism are close to each other, regardless of the radiation model, for a range of scalar dissipation rates. Results obtained with the one-step mechanism deviate more strongly, confirming that a one-step mechanism is not a good choice to predict extinction due to dilution of air. An important finding of the study is that the constant radiative fraction model fails to predict a low scalar dissipation rate extinction limit, which the RADCAL-based model does predict. Considering the CO values, the results from the ARM2 and the Smooke mechanisms differ quite strongly, with relatively low values with the Smooke mechanism for the range of scalar dissipation rates. Results obtained from the GRI3 are very close to the ARM2 results (within 2%) and therefore it is possible to reduce the computational costs, by relying on the ARM2 mechanism.

KEYWORDS: Extinction, fire, flamelet, emissions.

INTRODUCTION

This study is part of a larger project, targeting the prediction of carbon monoxide emissions and extinction phenomena in underventilated compartment fires. As carbon monoxide is the leading cause of death in fire victims, there is a strong interest in the ability to predict emissions in compartment fires for safety reasons. The production of carbon monoxide in underventilated fires can be due to a number of factors. The diluted atmosphere alone in underventilated compartments

Proceedings of the Ninth International Seminar on Fire and Explosion Hazards (ISFEH9), pp. 89-99
Edited by Snegirev A., Liu N.A., Tamanini F., Bradley D., Molkov V., and Chaumeix N.
Published by St. Petersburg Polytechnic University Press
ISBN: 978-5-7422-6496-5 DOI: 10.18720/spbpu/2/k19-104

will enhance the production of carbon monoxide due to incomplete combustion. Extinction is another mechanism that contributes to the production of carbon monoxide, as unburnt fuel leaks into the ceiling layer of the compartment, where it then reacts to produce carbon monoxide. Furthermore, the activity in the ceiling layer is at low temperatures (i.e., 800 K), and therefore the chemistry is slow, bringing additional complexity to the combustion modelling and in the choice of the chemistry mechanism.

Another aspect which is important to consider in the simulation of fires, but often neglected in jet flame simulations, is radiation. As fires are buoyancy-driven and characterized by low velocities, the mixing times are much longer, and the scalar dissipation rates much smaller than in jets. In low scalar dissipation rate regions, radiative heat losses are higher, and this could eventually lead to extinction due to a large enough drop in temperature [8]. Because of these phenomena, one also has to consider the extinction limit at low scalar dissipation rates in fires, and this limit is the focus of the current study.

Because extinction, re-ignition and finite-rate chemistry effects need to be considered, a combustion model that is able to account for these is required. This led to the choice of the Conditional Moment Closure (CMC) method [9]. CMC is a high-end model, that accounts for finite-rate chemistry effects [10] and was used previously to simulate extinction in jet flames [11,12]. Furthermore, as opposed to the flamelet-based models, CMC is well suited for the prediction of carbon monoxide emissions in compartment fires due to the presence of the transport in space in the equations, by which CMC is able to model the situation where CO is formed in the high temperature plume and then transported to non-reactive parts of the flow [13]. It is the aim of this research to apply LES-CMC for the prediction of extinction and carbon monoxide emissions in fires, which, to the best of the author's knowledge, has not been reported so far.

As extinction and carbon monoxide emissions are highly dependent on the choice of the chemical mechanism and radiation model, the present study has been conducted in order to evaluate the impact of different chemistry mechanisms and radiation models on extinction in the low scalar dissipation rate limit. The case study corresponds to a 0D reactor flow computation (CMC-0D), as no transport in physical space is taken into account, and it concerns a numerical study by means of the unsteady laminar flamelet approach in mixture fraction space. This is the first step towards applying the CMC model to simulate compartment fires. A similar study with the CMC-0D code was conducted by Stankovic et al [6], in which the effects of the transport in space were neglected, and the impact of different chemistry mechanisms was studied, on auto-ignition.

Four chemistry mechanisms are compared, namely a one-step global mechanism [1], Smooke [2], ARM2 [3] and the GRI3 mechanism [4]. The GRI3 is the most detailed mechanism, and the one-step mechanism is the simplest one. The study on the carbon monoxide emissions is done using the Smooke, ARM2 and GRI3 mechanism, as the one-step mechanism applied does not provide CO emissions. The four chemistry mechanisms are combined with two different radiation models, which are often applied in fire simulations: an optically thin model with radiative properties based on the RADCAL model and a constant radiative fraction model. These two models are then compared to cases without radiation, in order to evaluate the impact of radiation in different simulated cases.

The test case under study is based on the UMD line burner (Fig. 1), developed at the University of Maryland [7]. It allows the assessment of different modelling approaches in the simulation of extinction. It features a buoyant, turbulent, methane-fueled diffusion flame, with a controlled, diluted co-flow. The coflow is the oxygen/nitrogen mixture, by which extinction is achieved through the increase of the nitrogen mass fraction. The UMD line burner is a target case of the IAFSS MaCFP (Measurement and Computation of Fire Phenomena) workshop series [14, 15]. The present study does not involve CFD. The settings applied in the present CMC-0D reactor flow

computations are chosen in agreement with the fuel and oxidizer composition, as well as the anticipated range of scalar dissipation rates.

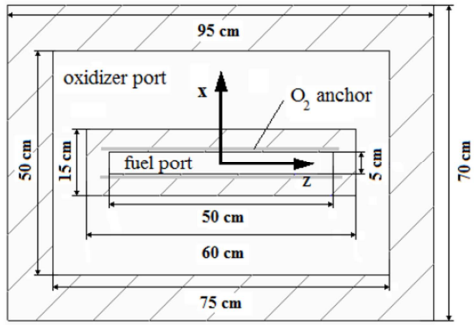

Fig. 1. Top view of the burner, co-flow and oxygen anchor outlet, redrawn after Ref. [16].

CMC-0D EQUATIONS

The computations are conducted using a stand-alone CMC-0D code [6]. In the code, pressure is fixed at 101 325 kPa, as no pressure equation is solved, nor momentum or mass conservation equations. Density is calculated from pressure, temperature and species concentrations. The difference between the CMC-0D equations and the general CMC equations is that transport in space is not solved with the CMC-0D model, which makes it essentially an unsteady laminar flamelet model. The equations are solved for conditionally averaged reacting scalars, conditioned on the mixture fraction ξ, as $Q_i = \langle Y_i|\xi = \eta\rangle = \langle Y_i|\eta\rangle$, where η is the sample space variable for the conserved scalar ξ and the operator $\langle\cdot\,|\xi = \eta\rangle$, briefly $\langle\cdot\,|\eta\rangle$, denotes ensamble averaging subjected to the fulfillment for the condition at the right-hand side of the vertical bar. The equations are solved for all N species of the reaction mechanism and temperature:

$$\frac{\partial Q_i}{\partial t} = \langle N|\eta\rangle \frac{\partial^2 Q_i}{\partial \eta^2} + \langle W_i|\eta\rangle \,, \tag{1}$$

$$\frac{\partial Q_T}{\partial t} = \langle N|\eta\rangle \left[\frac{1}{c_{p\eta}}\left(\frac{\partial c_{p\eta}}{\partial \eta} + \sum_{i=1}^{n} c_{p,i_\eta} \frac{\partial Q_i}{\partial \eta}\right)\frac{\partial Q_T}{\partial \eta} + \frac{\partial^2 Q_T}{\partial \eta^2}\right] - \frac{1}{c_{p_\eta}}\left(\left\langle \sum_{i=1}^{n} h_i W_i \,\middle|\, \eta \right\rangle + \langle q_r|\eta\rangle\right) \tag{2}$$

where $\langle q_r|\eta\rangle$ is the conditional heat loss due to radiation and $c_{p_\eta} = \langle c_p|\eta\rangle$ is the conditional specific heat capacity at constant pressure.

The conditional reaction rates $\langle W_i|\eta\rangle$ are obtained from the conditionally averaged species and temperature, as in first-order CMC:

$$\langle W_i|\eta\rangle = W_i(Q_i, Q_T) \,. \tag{3}$$

Unless mentioned otherwise, the conditional scalar dissipation rate $\langle N|\eta\rangle$ is modelled with the Amplitude Mapping Closure (AMC) model [17], which has a bell shape, labeled as function $G(\eta)$. This is representative of the conditional scalar dissipation rate in a counter-flow configuration. The conditional scalar dissipation rate is modelled as follows:

$$\langle N|\eta\rangle = N_0 G(\eta), \tag{4}$$

where

$$G(\eta) = exp\left(-2\left(erf^{-1}(2\eta - 1)\right)^2\right) \quad (5)$$

and (6)

$$N_0 = \frac{N}{\int_0^1 G(\eta)P(\eta)d\eta}$$

The model in CMC-0D is implemented as

$$\langle N|\eta\rangle = exp\left(-2\left(erf^{-1}(2\eta - 1)\right)^2\right) N_{max} \quad (7)$$

where erf^{-1} is the inverse error function, and N_{max} is maximum value of the scalar dissipation rate, which is imposed at $\eta = 0.5$.

The equations are solved in mixture fraction space, in the range [0:1], which is discretized into a number of bins, i.e. computational mesh in mixture fraction space, clustered around the stoichiometric mixture fraction.

CHEMISTRY MECHANISM

Four chemistry mechanisms are compared. The one-step global mechanism reads [1]:

$$CH_4 + 2O_2 \rightarrow CO_2 + 2H_2O \quad (8)$$

$$r_1 = 3 * 10^{22} exp(-4.5 * 10^4/RT)[CH_4][O_2]^2 \quad (9)$$

where r_1 is the reaction rate, R is the molar gas constant, T is the temperature and $[CH_4]$ and $[O_2]$ are the methane and oxygen concentration respectively.

The 'Smooke' mechanism [2] consists of 16 species and 25 chemical reactions, the 'ARM2' mechanism [3] consists of 19 species and 15 reactions, while the 'GRI3' mechanism [4] is the most complex and consists of 53 species and 325 reactions.

RADIATION MODELING

Considering radiation, two radiation models are compared: an optically thin model, with radiative properties based on the RADCAL model by Grosshandler [5], and a constant radiative fraction model. With the former model, the conditional heat loss due to radiation per unit volume $\langle q_r|\eta\rangle$ is calculated as:

$$\langle q_r|\eta\rangle = 4\sigma\kappa(Q_T^4 - T_0^4) \quad (10)$$

where σ is the Stefan-Boltzmann constant, Q_T is the local temperature and T_0 is the background temperature, $T_0 = 298\ K$ in this study. The Planck mean absorption coefficient $\kappa = p_{H_2O} * a_{p,H_2O} + p_{CO_2} * a_{p,CO_2} + p_{CH_4} * a_{p,CH_4} + p_{CO} * a_{p,CO}$, where $a_{p,i}$ is the Planck mean absorption of species i and p_i is its partial pressure. Curve fits for the mean absorption coefficients are found in [18].

For H_2O, CH_4, CO and CO_2 they correspond to expressions of the type $a_{p,i} = c0 + c1 * \left(\frac{1000}{Q_T}\right) + c2 * \left(\frac{1000}{Q_T}\right)^2 + c3 * \left(\frac{1000}{Q_T}\right)^3 + c4 * \left(\frac{1000}{Q_T}\right)^4 + c5 * \left(\frac{1000}{Q_T}\right)^5$. The coefficients are found in Table 1. For CO, they depend on temperature, as shown in the table. Soot is not taken into account, as the effects of soot on the overall radiative heat loss were reported to be small [19].

Table 1. Coefficients for H_2O, CO_2, CH_4 and CO.

	H_2O	CO_2	CH_4	CO, $T < 750K$	CO, $T \geq 750K$
c0	-0.23093	18.741	6.6334	4.7869	10.09
c1	-1.12390	-121.310	-0.0035686	-0.06953	-0.01183
c2	9.41530	273.500	1.6682	2.95775	4.7753
c3	-2.99880	-194.050	-0.8	-4.25732	-5.87209E-10
c4	0.51382	56.310	2.5611E-10	2.02894E-10	-2.5334E-14
c5	-1.86840E-05	-5.8169	2.6558e-14E-14	0	0

On the other hand, when using the constant radiative fraction model, the radiative source term is obtained as:

$$\langle q_r|\eta\rangle = \chi_{rad}\langle \dot{\omega}_{h_s}'''|\eta\rangle \tag{11}$$

where $\langle \dot{\omega}_{h_s}'''|\eta\rangle$ is the conditional local heat release rate per unit volume and χ_{rad} is the radiative fraction obtained from the experiments. In [20], the global radiative fraction has been reported for the UMD line burner as function of the oxygen concentration in the oxidizer. These experimentally obtained values have been used in the simulations here.

CASE SET-UP

As mentioned, the test case corresponds to the UMD line burner (Fig. 1). The fuel is pure methane, and the oxidizer is an oxygen/nitrogen mixture. The simulations have been conducted for the four chemistry mechanisms and the two radiation modelling approaches, as described above. Results are also compared to simulations without radiation, for a range of imposed maximum scalar dissipation rates N_{max}, in Eq. (7). The values of N_{max} vary from 0.2 s^{-1} to 2.0 s^{-1}, which was the range of values along the centerline of the flame in CMC-3D simulations of the UMD line burner, conducted by the authors, as no such information was available in the experimental results. . Furthermore, a constant conditional scalar dissipation rate over the entire mixture fraction range has been imposed, in order to evaluate the impact of the conditional scalar dissipation rate profile shape on extinction. The shapes of the two approaches are illustrated in Fig. 2.

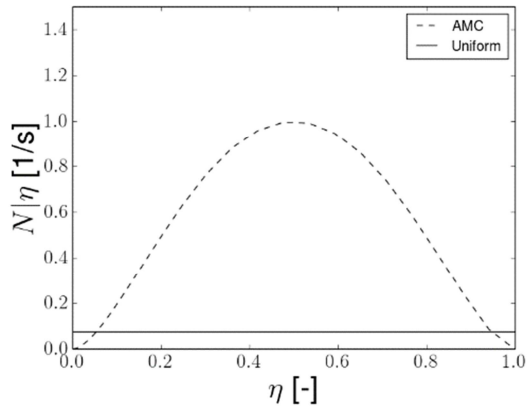

Fig 2. Profiles for the conditional scalar dissipation rate, with the AMC model and a uniform distribution model with an imposed value as that of the AMC model at stoichiometric mixturefraction.

The comparison between the AMC and uniform distribution models was done such that first the simulations with the AMC model were done. The values of the scalar dissipation rate obtained with the AMC models at stoichiometric conditions, at the oxygen mass fraction at which extinction occurs, were then imposed at all mixture fraction values using the uniform model. For each case, starting from air as oxidizer, the amount of N_2 in the oxidizer is increased in independent simulations, until extinction is reached. The target was to obtain the oxygen mass fractions accurate to the third decimal, and so the increase in N_2 was by steps of 0.001 mass fractions of N_2 when approaching the extinction values, until extinction occurred. The computational mesh consists of 50 bins in mixture fraction space, unless specified otherwise.

RESULTS

An important quantity to assess extinction is the value of O_2 mass fraction in the oxidizer for which extinction is observed. This is labeled as '$O_{2,ext}$' below. In the simulations, this value has been obtained through the incremental increase of N_2 in the oxidizer, as mentioned. The higher the value of $O_{2,ext}$, the quicker extinction is observed.

In Fig. 3, the maximum temperature as function of the maximum scalar dissipation rate (N_{max}), is shown for the ARM2, Smooke and one-step mechanism. The cases feature air as the oxidizer, and the imposed value of the radiative fraction χ=0.235, in the constant radiative fraction model. This is the value of radiative fraction, obtained from experiments for the UMD line burner, for cases where oxygen is air. From the results, it is interesting to note that only when the RADCAL-based radiation model is used, the temperature drop at low scalar dissipation rates is predicted. This is not captured by the constant radiative fraction model. Furthermore, as the scalar dissipation rate is increased, the maximum temperature obtained with the RADCAL-based model is getting very close to the value predicted in cases without radiation. This is consistent with the observation, that radiation has more impact at low scalar dissipation rates, and almost negligible at high scalar dissipation rates. This is why radiation is often neglected in jet simulations, while being very significant in fires.

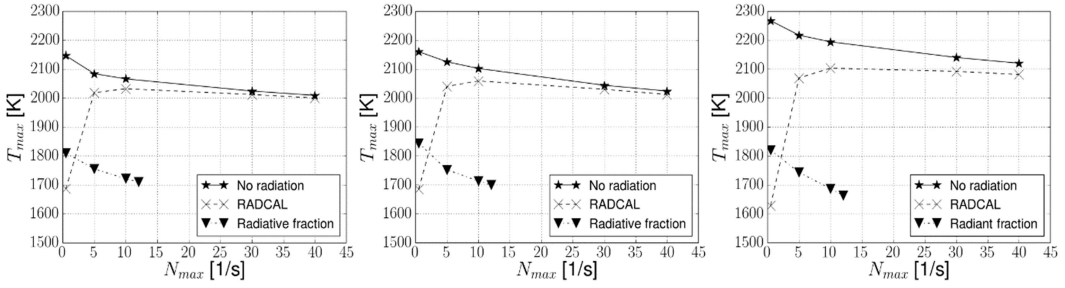

Fig. 3. Maximum temperature in mixture fraction space as function of the maximum scalar dissipation rate, for the (a) ARM2, (b) Smooke and (c) one-step global mechanism.

Fig. 4 shows the oxygen mass fraction at extinction for the one-step, Smooke and the ARM2 chemical mechanisms and different approaches for radiation. The results obtained with the radiative fraction model in Fig. 4 are obtained with two approaches: by setting the radiative fraction to be χ=0.235 in all cases, and the second with radiative fraction values taken from the experiments [19]. The values of the radiative fractions used at extinction, as obtained from experiments, are shown in Table 2. The difference between the mechanisms comes from the fact that the radiative fraction depends on the oxygen mass fractions $O_{2,ext}$, which is different for the mechanisms shown. As the radiative fraction is very low near extinction, the primary mechanism for extinction in the UMD line

burner is due to dilution of the oxidizer. The results when radiation is not taken into consideration and when the radiative fraction model is used, follow the same trend, either by setting a fixed value of the radiative fraction for all scalar dissipation rates or by taking the values from the experiments. Using χ=0.235, as expected, the decrease in temperature due to the radiative losses, leads to higher values of $O_{2,ext}$ (i.e., more prone to extinction), as compared to cases without radiation. When the radiative fraction is taken from the UMD line burner experiments however, the values of the oxygen mass fraction at extinction are nearly identical. The reason for such behaviour can be found in the experiments, since the radiative fraction decreases with decreasing oxgen mass fraction values, and therefor the radiative heat loss, through Eq. (11) will also decrease, making the term in most of the cases negligible at low levels of the oxygen mass fraction. As the scalar dissipation rate is increased, the values of the oxygen mass fraction at which extinction occurs are higher, and therefor, the effect of the source term, using the constant radiant approach will become more significant, which explains the deviation in Fig. 4 (c). The one-step mechanism is more sensitive than the ARM2 and Smooke mechanisms, which is also reflected in the results with the RADCAL-based model.

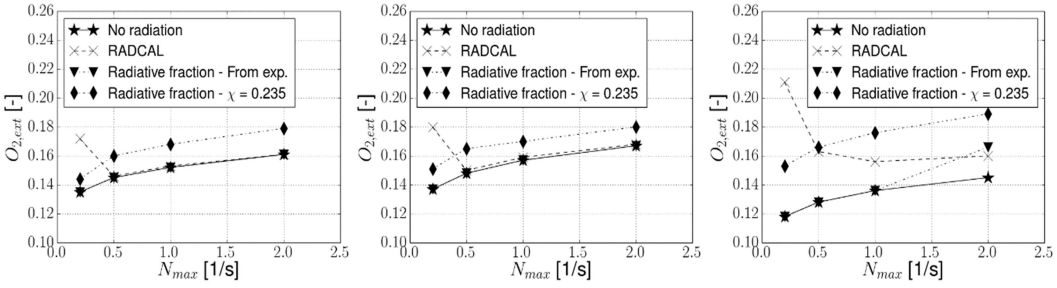

(a) (b) (c)

Fig. 4. The oxygen mass fraction at extinction ($O_{2,ext}$) as function of the maximum scalar dissipation rate with the (a) ARM2, (b) Smooke and (c) one-step global mechanisms.

Table 2. Radiative fractions with different chemistry mechanisms

N_{max} (1⁄s)	ARM2	Smooke	One-step
2.0	0.155	0.165	0.163
1.0	0.138	0.147	0.07
0.5	0.127	0.131	0
0.2	0.065	0.080	0

The comparison between the ARM2 and GRI3 mechanism (Fig. 5) shows that the results are very close for cases with no radiation, and using the RADCAL-based model, for a range of scalar dissipation rates (within 1.6% difference).

The influence of the shape of the different scalar dissipation rate on the oxygen mass fraction at extinction is shown in Fig. 6. Only the results with the ARM2 mechanism are shown, although the other mechanisms have shown such sensitivty as well, apart from the GRI3 mechanism, which remains to be investigated in this regard. As it can be seen, the shape does not have an impact on extinction due to dillution, only the value of the scalar dissipation rate at stoichiometry. When the RADCAL-based model is used however, there is a strong influence of the shape, in the low scalar dissipation rate cases.

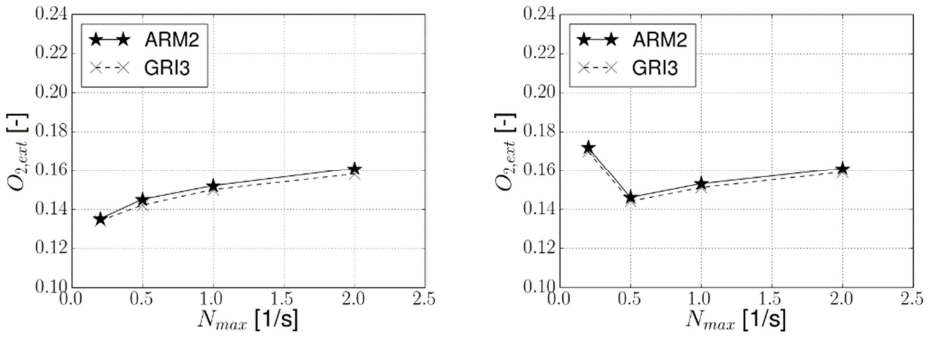

(a) (b)

Fig. 5. The oxygen mass fraction at extinction ($O_{2,ext}$) as function of the maximum scalar dissipation rate using the ARM2 and GRI3 mechanisms, in the case (a) without radiation and (b) with the RADCAL-based model

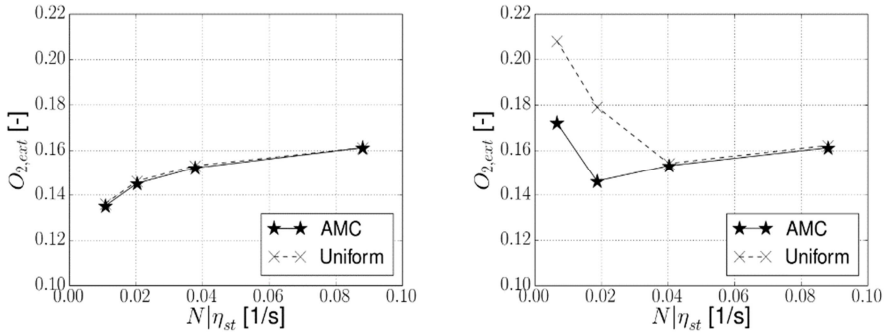

(a) (b)

Fig. 6. The oxygen mass fraction at extinction ($O_{2,ext}$) as function of the stoichiometric scalar dissipation rate, using the AMC and the uniform distribution models, coupled with the ARM2 mechanism, in the case with (a) the RADCAL-based model and (b) without radiation.

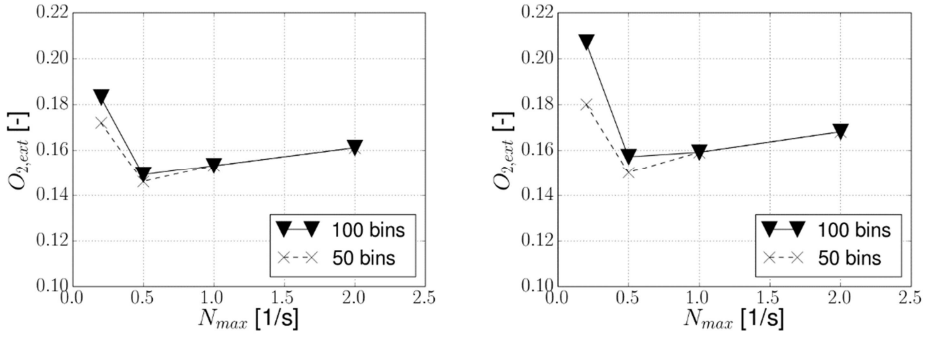

(a) (b)

Fig. 7. Impact of the number of bins on the oxygen mass fraction at extinction as function of the maximum scalar disipation rate, using the RADCAL-based model and the (a) ARM2 and (b) Smooke mechanisms.

The impact of the computational mesh (i.e., number of bins in mixture fraction space), on the value of the oxygen mass fraction at extinction was studied as well. Using the constant radiative fraction approach as well as in cases without using radiation, there was no effect on extinction beyond 50 bins (not shown). Only using the RADCAL-based model, the sensitivity is much larger and more

pronounced at low scalar dissipation rates (Fig. 7). The relative difference at $N_{max} = 0.5$ s^{-1} is about 22.6% and at $N_{max} = 0.2$ s^{-1}, it is 21%. This phenomenon is observed when either the Smooke or the ARM2 mechanisms are used. The one-step mechanism with the RADCAL-based model did not show sensitivity to the number of bins, beyond 50 bins, and the bin convergence study with the GRI3 mechanism is yet to be conducted. Therefore, when using the latter radiation model with mixture fraction based models and detailed chemistry, the impact on the number of bins at low scalar dissipation rate is important to take into account.

The maximum value of the carbon monoxide mass fraction in mixture fraction space, as function of the scalar dissipation rate is shown in Fig. 8. The difference between the ARM2 mechanisms results and GRI3 is within 2%, for a range of the scalar dissipation rates, using the RADCAL-based model and the approach without radiation. On the other hand, the difference between GRI3 and Smooke, can be as high as around 28%, using the RADCAL-based model and in cases without radiation, and it doesn't get lower than 11% (which was obtained in the case without radiation in Fig 8. (a), at max. scalar dissipation rate of 40).

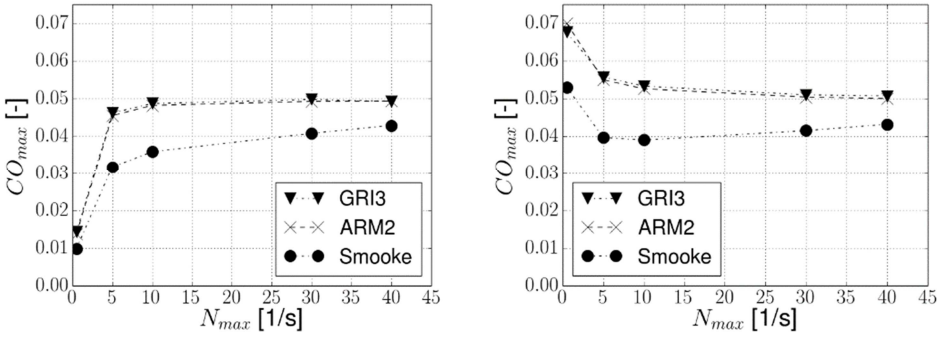

(a) (b)

Fig. 8. Comparison of the maximum value of CO mass fraction, in mixture fraction space, as function of the maximum scalar dissipation rate, obtained by the GRI3, ARM2 and Smooke mechanism. The computed cases are (a) without radiation and (b) with the RADCAL-based model

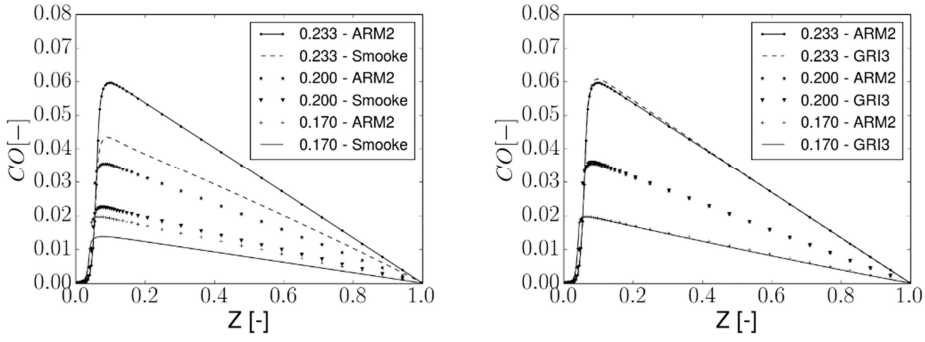

(a) (b)

Fig. 9. Comparisons of the carbon monoxide distributions in mixture fraction space without considering the influence of radiation using (a) the ARM2 and Smooke mechanisms and (b) the ARM2 and GRI3 mechanisms. Values in the legend refer to O_2 mass fraction in the oxidizer.

In Fig 9, the distributions of the carbon monoxide mass fraction in mixture fraction space are shown for different levels of oxygen mass fractions in the oxidizer. The carbon monoxide mass fractions

predicted using the Smooke mechanism are systematically lower than those predicted using the ARM2 mechanism, also for different oxygen concentrations in the oxidizer. Fig. 9 is for cases when radiation was not considered, however a similar trend was observed with the RADCAL-based model as well. The comparisons between the ARM2 and the GRI3 (Fig. 9(b)), show that the carbon monoxide mass fractions match very well, for different values of oxygen mass fractions in the oxidizer.

CONCLUSIONS

Comparing the four chemical mechanisms, the oxygen mass fraction values at extinction obtained with the multi-step mechanisms are close, while the one-step mechanism differs strongly, confirming that the one-step mechanism is not suitable to model extinction due to dilution of air. With respect to the calculation time, the GRI3 is the most expensive, followed by the ARM2 and Smooke, which were very close in terms of calculation time. The results from the study concerning the RADCAL-based model show that the impact of radiation increases with decreasing scalar dissipation rates. As the scalar dissipation rate is lowered the onset of extinction occurs at a higher oxygen mass fraction, or sooner than in cases when radiation is not included at all, or when using the radiative fraction model. An important finding is that the radiative fraction model fails to predict a low scalar dissipation rate extinction limit, which the RADCAL-based model does predict. Furthermore, it was found that there is a significant impact of the computational grid on extinction, when using the RADCAL-based model with the ARM2 and Smooke mechanisms, in low scalar dissipation rate cases. The shape of the scalar dissipation rate, used with the ARM2, Smooke or the one-step mechanisms and the RADCAL-based model also had an effect on extinction in low scalar dissipation rate cases. In the case of the one-step mechanism, the effect was observed even at higher values of the scalar dissipation rates.

Considering the carbon monoxide emissions, it is clear that there are large differences in the results obtained with the Smooke and the ARM2 mechanisms and that the choice of the mechanism is significant. This was observed for a range of scalar dissipation rates, and oxygen mass fraction levels in the oxidizer stream. On the other hand, the differences between the more detailed chemical mechanisms, the GRI3 mechanism and ARM2 are small, both for extinction and carbon monoxide emissions. Therefore, it is possible to use the much cheaper ARM2 mechanism, and thus reduce the computational cost.

ACKNOWLEDGEMENTS

This research has been funded by Ghent University (Belgium) through GOA project BOF16/GOA/004.

REFERENCES

[1] P. Bitala, M. Kozubková, P. Kadeřábek, V. Nevrlý, J. Dlabka, E. Kozubek, O. Štěpánek, M. Bojko, P. Kubát, Z. Zelinger, Experimental investigations and numerical simulations of methane cup-burner flame, InEPJ Web of Conferences 2013, Vol. 45, p. 01067, EDP Sciences, 2013.

[2] M.D. Smooke, Reduced kinetic mechanisms and asymptotic approximations for methan-air flames, Lecture Notes in Physics 384, 1991.

[3] Q. Tang, Computational modelling of turbulent combustion with detailed chemistry, PhD Thesis, Cornell University, 2003.

[4] G.P. Smith, D.M. Golden, M. Frenklach, N.W. Moriarty, B. Eiteneer, M. Goldenberg, C.T. Bowman, R.K. Hanson, S. Song, W.C. Gardiner, Jr., V.V. Lissianski, http://combustion.berkeley.edu/gri-mech/index.html

[5] W.L. Grosshandler, RADCAL: a narrow-band model for radiation calculations in a combustion environment, NIST Tech. Note 1402, 1993.

[6] I. Stankovic, B. Merci, Analysis of auto-ignition of heated hydrogen-air mixture with different detailed reaction mechanisms, Combust. Theory and Model. 15 (2011) 409-436.

[7] https://github.com/MaCFP/macfp-db/tree/master/Extinction/UMD_Line_Burner (accessed 10 July 2018)

[8] S.H. Chan, J.Q. Yin, B.J. Shi, Structure and extinction of methane-air flamelet with radiation and detailed chemical kinetic mechanism, Combus. Flame 112 (1998) 445-456.

[9] A.Y. Klimenko, R.W. Bilger, Conditional moment closure for turbulent combustion, Prog. Energy Combust. Sci. 25 (1999) 595-687.

[10] A. Garmory, E. Mastorakos, Capturing localised extinction in Sandia Flame F with LES–CMC, Proc. Combust. Inst. 33 (2011) 1673-1680.

[11] S. Ayache, E. Mastorakos, Conditional Moment Closure/Large Eddy Simulation of the Delft-III natural gas non-premixed jet flame, Flow Turb. Combust. 88 (2012) 207-231.

[12] H. Zhang, A. Garmory, D.E. Cavaliere, E. Mastorakos, Large Eddy Simulation/Conditional Moment Closure modeling of swirl-stabilized non-premixed flames with local extinction, Proc. Combust. Inst. 35 (2015) 1167-1174.

[13] M.J. Cleary, CMC modelling of enclosure fires, PhD Thesis, University of Sydney, 2004.

[14] www.iafss.org/macfp/

[15] B. Merci, J.L Torero, A. Trouve, Call for participation in the first workshop organized by the IAFSS Working Group on Measurement and Computation of Fire Phenomena, Fire Saf. J. 82 (2016) 146-147.

[16] S. Vilfayeau, J.P. White, P.B. Sunderland, A.W. Marshall, A. Trouvé, Large eddy simulation of flame extinction in a turbulent line fire exposed to air-nitrogen co-flow, Fire Saf. J. 86 (2016) 16-31.

[17] E.E. O'Brien, T.L. Jiang, The conditional dissipation rate of an initially binary scalar in homogeneous turbulence, Phys. Fluids A: Fluid Dynamics 3 (1991) 3121-3123.

[18] https://www.sandia.gov/TNF/radiation.html

[19] S. Vilfayeau, Large eddy simulation of fire extinction phenomena, PhD Thesis, University of Maryland, College Park, 2015.

[20] J.P. White, E.D. Link, A.C. Trouvé, P.B. Sunderland, A.W. Marshall, J.A. Sheffel, M.L. Corn, M.B. Colket, M. Chaos, H.Z. Yu, Radiative emissions measurements from a buoyant, turbulent line flame under oxidizer-dilution quenching conditions, , Fire Saf. J. 76 (2010) 74-84.